3rd Biennial International Conference on Powertrain Modelling and Control (PMC 2016)
Testing, Mapping and Calibration
7th-9th September 2016, Loughborough University, UK

Analysis of Lubricated Contact in Continuously Variable Transmissions (CVT)

Medina Huerta, I. , Mohammadpour, M. and Rahnejat, H.*

Wolfson School of Mechanical Engineering, Loughborough University, LE113TU

**Corresponding author: i.medina-huerta-13@student.lboro.ac.uk*

Abstract: This paper presents a tribological model for a toroidal CVT. The model predicts the lubricant film thickness, viscous and boundary generated friction and the spin power loss in the contact. This is in order to evaluate the effect of different parameters on the efficiency and durability of the CVT system. An optimisation study is carried out to ascertain the effect of contact surface materials, lubricant rheology and contact geometry upon power loss and maximum generated contact pressure. The results show that numerically, even if the contact pressure cannot be significantly reduced, the contact spin power loss can be reduced by as much as 24%., thus improving system efficiency

Keywords— Continuously Variable Transmissions (CVT), durability, efficiency, lubrication, optimisation

1. Introduction

Continuously variable transmission (CVT) is a gearless and step-less transmission system which theoretically provides an infinite number of transmission ratios. It also facilitates the ability of a vehicle to cruise at an optimum efficiency point of the engine. The system is a good replacement for the conventional gearbox in vehicles. However, the system itself is far too inefficient compared with various alternatives. Challenging new governmental regulation for low carbon emissions, coupled with the widespread use of automatic transmissions has added impetus for further research and development into CVT.

The toroidal CVT is the most widely used configuration, which comprises several components, rotating around different axes. When in motion, the disk and the roller touch at the contact point, where an elastohydrodynamic (EHL) lubricant film is expected to form. Owing to the usual thinness of the lubricant film, the spinning contact is subjected

to viscous and boundary friction. The spinning motion contributes to undesired power loss, which leads to lower operational energy efficiency.

An understanding of kinematics of contact is essential for the tribological assessment of the system. Under given conditions, prediction of load carrying capacity, film thickness, Stribeck's oil film parameter, viscous and boundary friction, maximum pressure, and power loss due to spin velocity are required and presented in this paper.

Chittenden and Dowson's [1] film thickness equation is used in order to predict the minimum and central contact lubricant film thickness under elastohydrodynamic lubrication (EHL). Furthermore, to predict fiction, Johnson and Evans [2] and Greenwood and Tripp [3] approaches are used for the modelling of viscous friction and boundary friction respectively. Finally, the model also takes into account contact spin and its impact in terms of power loss.

A sensitivity analysis is carried out with respect to the choice of surface material, lubricant rheology and contact geometry to yield the least spin power loss and maximum contact pressure (load carrying capacity).

2.Toroidal CVT

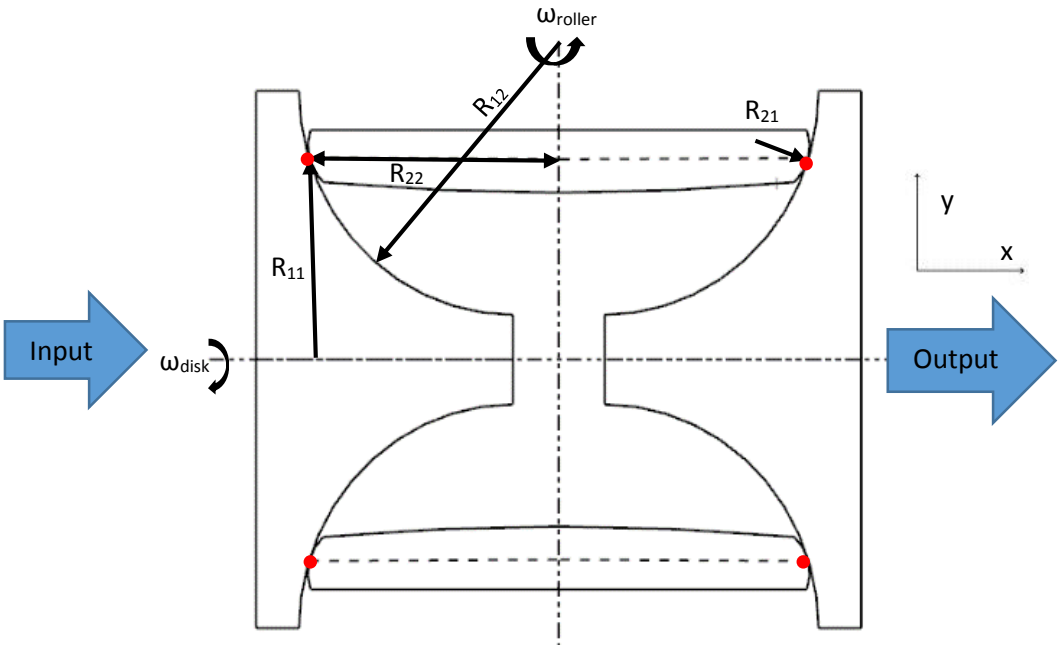

Figure 1 – Segment of toroidal CVT

Toroidal CVTs use disks and rollers as a way of transmitting power between the input and output shafts, which rotate around two axes, providing a variable transmission ratio.

Disk spin occurs around the *x*-axis and the rollers move in the *x*-*y* plane and spin along the y-axis (figure 1). This provides the opportunity contact with the different parts of the disks groove, and so offering a large range of possibilities in term of the transmission ratio. Most systems are composed of two sets of two disks, or two whole grooves, in which 2 to 3 rollers are equidistantly placed around the 360 degrees toroid.

Figure 1 shows the side-view of half a toroidal CVT, which comprises two rollers in the cavity. The EHL contact is located between the rollers and the disks, marked with red dots on Figure 1.

3. Methodology

The main problems with any kind of CVT and especially the toroidal configuration are durability and power loss. Durability depends on the generated contact pressure leading to sub-surface stresses which may cause exceed their elastic limit of $\tau_{max} = 0.31p_0 \geq 0.5\sigma_Y$ (in the case of maximum sub-surface shear stress) according to the Tresca criterion [4], where σ_Y is the material yield stress or alternatively with the equivalent stress, $\sigma_e = 2|\tau_{zxmax}/P_h| > 0.5$, according to the maximum reversing shear stress criterion [5,6]. The generated pressure depends on the normal applied contact load able to transmit the required torque due to the generated contact friction. In order to calculate the correct value for the normal load, total friction including viscous and boundary components should therefore be determined. On the other hand, with regard to system efficiency, a kinematic study of the contact is made in order to obtain the spin velocity and its resultant power loss.

3.1. Tribological Model

3.1.1. Fiction

In order to determine the total friction, the addition of viscous and boundary friction components is required. Contact friction should then be sufficient to transmit the applied torque at the instantaneous contact point. The total friction comprises viscous and boundary term as:

$$F_{total} = F_v + f_b \tag{1}$$

i. Viscous friction

For viscous friction, the method used is due to Evans and Johnson [2], which covers lubricant shear in Newtonian as well as non-Newtonian behavior. The equations embody their traction maps, and for this case represented by areas II and III.

Furthermore, they have other equations for the other areas within the map, but they are not of the interest in this paper. Therefore, in order to find viscous friction:

$$F_v = W \times \left[0.87\, \bar{\alpha}\bar{\tau}_0 + 1.74 \frac{\bar{\tau}_0}{\bar{p}}\, ln\left\{ \left\{ \frac{1.2}{\bar{\tau}_0 h_0} \left(\frac{2k\eta_0}{1 + 9.6\xi} \right) \right\} \right\}^{1/2} \right] \quad (2)$$

Where W is the normal force in the contact and the parameter ξ is [2] given as:

$$\xi = \frac{k}{h_0} \left(\frac{16\bar{p}R'}{\pi E_r k' \rho' c' U} \right)^{1/2} \quad (3)$$

It is noteworthy that even though these equations are predominantly used for line contact geometry, they are suitable for elliptical contacts as well.

ii. Boundary Friction

The Greenwood and Tripp [3] model is used for evaluation of boundary friction contribution. This is based on the Stribeck oil film parameter, essentially indicating the proportion of load carried by the asperities. This key parameter is calculated as follows:

$$\lambda = \frac{h_0}{\sigma} \leq 3 \quad (4)$$

where, σ is the composite or convoluted root mean square roughness of the counter face surfaces.

Due to a thin lubricant film, a proportion of the load is carried by the asperities, however a small proportion this may be in practice. The asperity share of carried load is [3]:

$$W_a = \frac{16\sqrt{2}}{15} \pi (\xi_1 \beta \sigma)^2 \sqrt{\frac{\sigma}{\beta}}\, E_r\, A\, F_{5/2}\,(\lambda) \quad (5)$$

$$E_r = \frac{\pi}{\left({(1 - \nu_1^2)}/{E_1} \right) + {(1 - \nu_2^2)}/{E_2}} \quad (6)$$

This relationship assumes Gaussian distribution of asperity heights on the counter faces, coming into contact. Therefore, it is accurate for fairly smooth surfaces or those after running-in wear.

For this specific case, one can assume that the roughness parameter $(\xi_1\beta\sigma)$ =0.055, and $F_{5/2}\ (\lambda)$ is a statistical function, representing the probability of asperity interactions for Gaussian distribution of the asperities. This can be represented by a polynomial fit [7, 8]:

$$F_{5/2}\ (\lambda) = \begin{cases} -0.004\lambda^5 + 0.057\lambda^4 - 0.296\lambda^3 + 0.784\lambda^2 - 1.078\lambda + 0.617 & ; for\ \lambda \leq 3 \\ 0 & ; for\ \lambda > 3 \end{cases} \quad (7)$$

In reality a thin film of lubricant is entrapped in the inter-asperity spaces or absorbed to their contacting summits, experiencing non-Newtonian shear, thus: [7]:

$$f_b = \tau_L A_a \quad (8)$$

τ_L in this case is the limiting shear stress of the lubricant [9]:

$$\tau_L = \tau_0 + \varepsilon P \quad (9)$$

And the average (Pascal pressure) for asperity contact is: $P = \frac{W_a}{A_a}$ (10)

The asperity contact area is found as [3]:

$$A_a = \pi^2 (\xi\beta\sigma)^2 A F_2(\lambda) \quad (11)$$

where, again F_2 is a statistical function [7, 8]:

$$F_2(\lambda) = \begin{cases} -0.002\lambda^5 + 0.028\lambda^4 - 0.173\lambda^3 + 0.526\lambda^2 - 0.804\lambda + 0.500 & ; for\ \lambda \leq 3 \\ 0 & ; for\ \lambda > 3 \end{cases} \quad (12)$$

3.1.2. Film Thickness

As equation (2) shows in order to find obtain friction, film thickness, h_0, should be determined.

This film thickness formulae for the lubricant film thickness for central film, h_0 is [1]:

$$H_{cen}^{*} = 4.31 U_e^{0.68} G_e^{0.49} W_e^{-0.073} \left\{1 - exp\left[-1.23 \left(\frac{R_s}{R_e}\right)^{2/3}\right]\right\} \quad (13)$$

$$h_0 = H_{cen}^{*} * R_e \quad (14)$$

where, R_e and R_s are auxiliary radii of curvature along and normal to **V** and defined as:

$$\frac{1}{R_s} = \frac{\sin^2\theta}{R_x} + \frac{\cos^2\theta}{R_y} \text{ and } \frac{1}{R_e} = \frac{\cos^2\theta}{R_x} + \frac{\sin^2\theta}{R_y} \quad (15)$$

The dimensionless groups are:

$$U_e = \frac{\pi \eta_0 \mathbf{V}}{4 E_r R_e} \quad (16)$$

$$W_e = \frac{\pi W}{2 E_r R_e^2} \quad (17)$$

$$G_e = \frac{2}{\pi}(E_r \alpha) \quad (17)$$

3.1.3. Spin power loss

To obtained the total contact power loss due to spin it is necessary to calculate the dimensions of the elliptical contact footprint (figure 2). Thus [4, 10]:

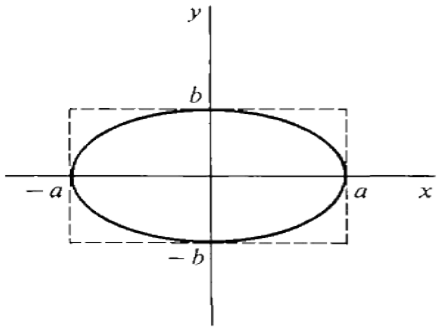

Figure 2 – Elliptical contact footprint

$$a = \left(\frac{6\bar{k}^2\bar{\varepsilon}WR'}{\pi\bar{k}Er}\right)^{1/3} \quad (19)$$

$$b = \left(\frac{6\bar{\varepsilon}WR'}{\pi\bar{k}Er}\right)^{1/3} \quad (20)$$

$$P_{max} = \frac{3W}{2\pi ab} \quad (21)$$

$$\bar{p} = \frac{W}{\pi ab} \quad (22)$$

$$\bar{\varepsilon} = 1.0003 + \frac{0.5968R_x}{R_y} \quad (23)$$

$$\bar{k} = 1.0339 + \left(\frac{R_x}{R_y}\right)^{0.0636} \quad (24)$$

Once the values are determined, a grid of size 100x100 is made to compute the "radius" vectors, *r(i,j)* at the centre of each element, then the local spin velocity becomes:.

$$dV = r(i,j) * \omega_{spin} \quad (25)$$

The elemental shear stress for each computational cell becomes:

$$\tau(i,j) = \frac{\eta_0 dV}{h_0} \quad (26)$$

And cell friction as:

$$F_{vcell} = \tau(i,j)A_{cell} \quad (27)$$

Thus, one can find the contact as:

$$P(i,j) = \sum_i \sum_j (F_{vcell}(i,j) * dV(i,j)) \quad (28)$$

3.2. Kinematic Model

A kinematic model is created to determine the angular spin velocity, ω_{spin}. The kinematic equation shown in figure 3 becomes:

$$\omega_{spin} = (\omega_{disk} \sin(f)) - (\omega_{roller} \cos(q)) \tag{29}$$

4. Results and Discussion

4.1. Model tribological outputs

The analysis is carried out in respect of the toroidal CVT with specifications listed in Table 1. The lubricant used is Santotrac 50 traction fluid with its rheological data also included in the table, as well as the other input parameters necessary for the analysis. The applied torque and speed are 40Nm and 2000rpm respectively.

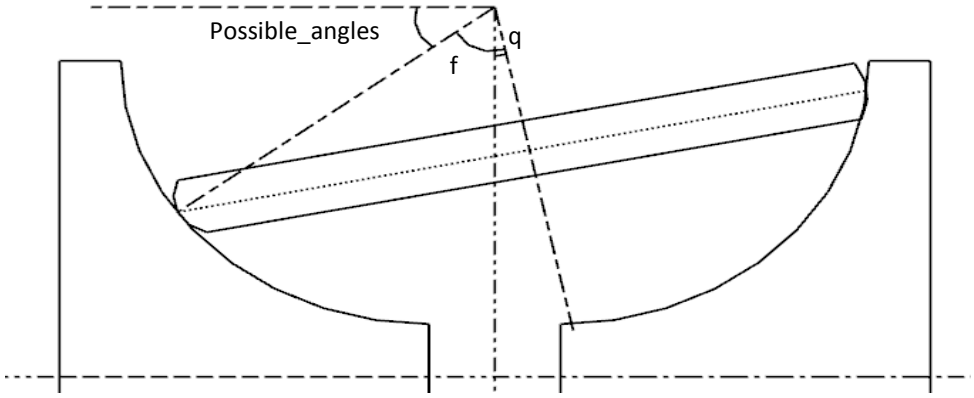

Figure 3 - Side view of the toroidal CVT and its angles for ω_{spin}

Symbol	Description	Value used	Units
α	Pressure-viscosity coefficient	1,71x10^{-08}	Pa^{-1}
$\bar{\alpha}$	Average pressure-viscosity coefficient	1,65x10^{-08}	Pa^{-1}
c'	Specific heat capacity of the solids	470	J/KgK
E	Minimum radius of the disk (mid-point)	0,025	m
E_1	Young's modulus of the first material	210	GPa
E_2	Young's modulus of the second material	210	GPa
$\bar{\eta}$	Average viscosity	0,0046	Pa. s
η_0	Entry viscosity of lubricant	0,01	Pa. s
k	Surface material thermal conductivity	46	W/mK
k'	Lubricant thermal conductivity	0,16	JKg/K
λ_{cr}	Critical Stribeck's oil film parameter	3	(-)
$n_{cpoints}$	Number of contact points in the system	6	(-)
$n_{rollers}$	Number of rollers in the system	3	(-)
R_{12}	Reduced radius of the disk	0,04	m
R_{21}	Reduced radius of the roller	0,02	m
R_{22}	Radius of the roller	0,032	m
R_{max}	Maximum radius of the disk	0,065	m
ρ'	Surface material density	7850	Kg/m^3
σ	Composite RMS Surface roughness	2	µm
T	Input Torque	[20:10:60]	Nm
τ_L	Limiting shear stress	3	MPa
$\bar{\tau}_0$	Average Eyring stress	2	MPa
θ	Angle of lubricant entrainment vector	90	Degrees
ν_1	Poisson's ratio of first material	0,3	(-)
V	Rolling speed in the y direction	0	m/s
ν_2	Poisson's ratio of the second material	0,3	(-)
ω_{disk}	Angular velocity of the input disk	[1500:500: 3000]/60	$revs/min$

Table 1: System data

The results are shown in figures 4 – 9. Figure 4 shows the required applied load to generate the necessary friction, depending on the angle, and to transmit the input torque. Results show that any increase in the required torque transmission has a significant implication for applied load requirement, but not as much with respect to sliding speed.

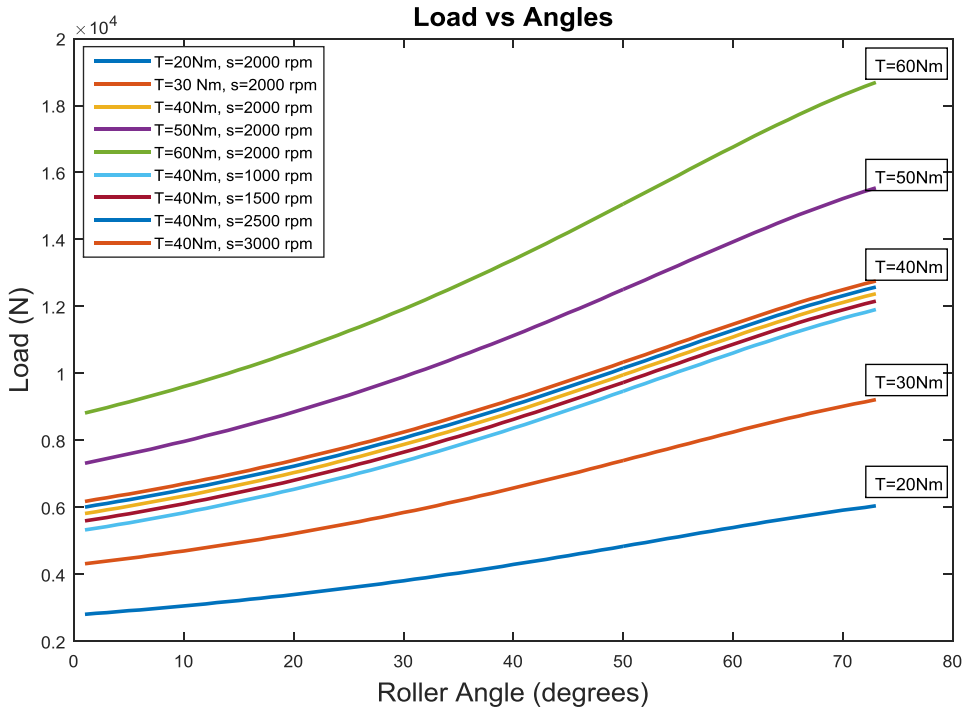

Figure 4- Variation of contact load with roller angle at different torques

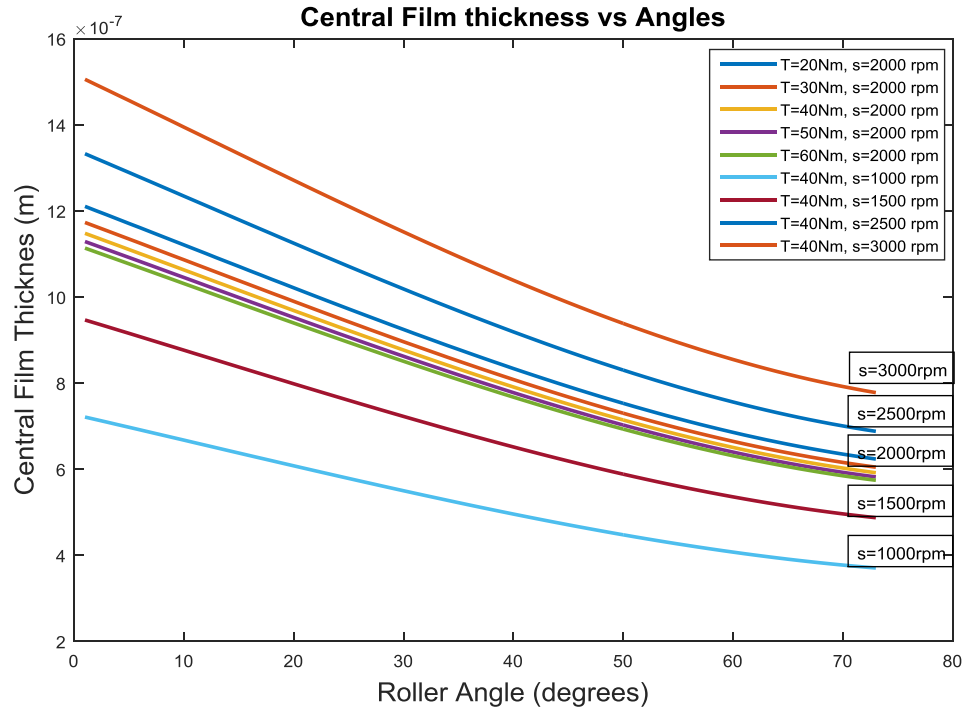

Figure 5- Variation of Central Film Thickness vs Roller angle for various conditions

Figure 5 shows the variation of central contact lubricant film thickness with applied torque and sliding speed. Clearly, the main effect is with speed under EHL conditions as shown in the results. An average lubricant film thickness of 11 micrometres is obtained. This is within the range of surface roughness, thus a mixed regime of lubrication is prevalent.

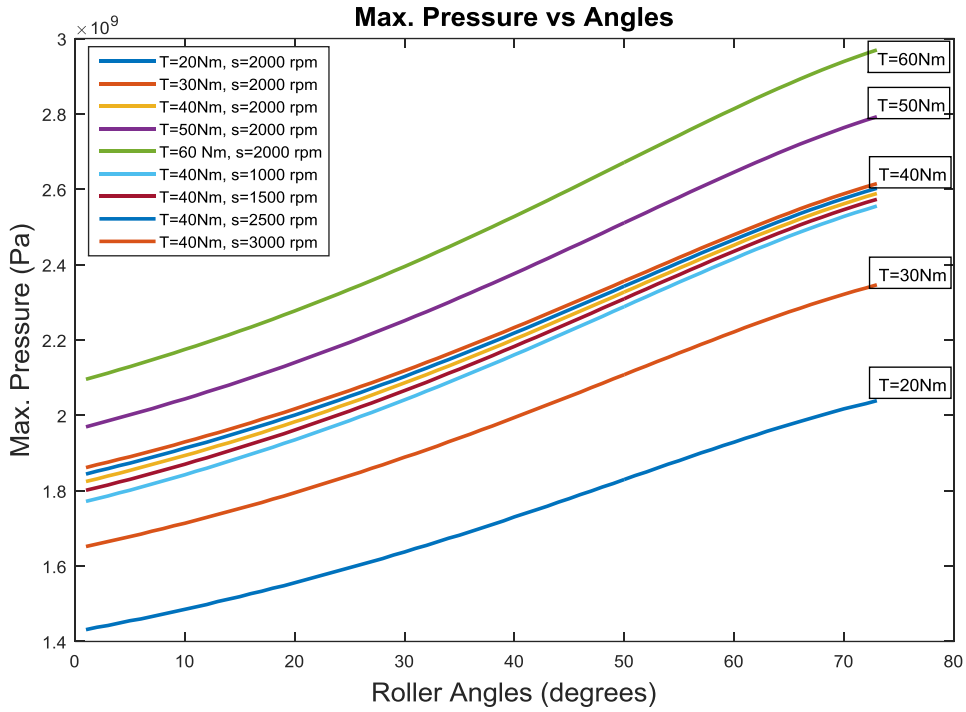

Figure 6- Maximum Pressure versus roller contact angles under various conditions

Figure 6 presents the maximum generated contact pressure. The maximum permissible pressure of the contact is around 1.6GPa for the chosen material, and to keep the system under optimal conditions this means that the maximum admitted torque should not exceed 60 Nm.

Figure 7 and 8 show the spin power loss due to generated friction. As the boundary friction contribution is relatively small, it barely plays a role in the total spin power loss. However, its behaviour shows that the smallest value is found in between 55º and 57º depending on the speed. For viscous friction the local minimum is located between 40º and 44º. Finally, for the highest speeds the power loss is at its maximum and can reach up to 2.5 kW.

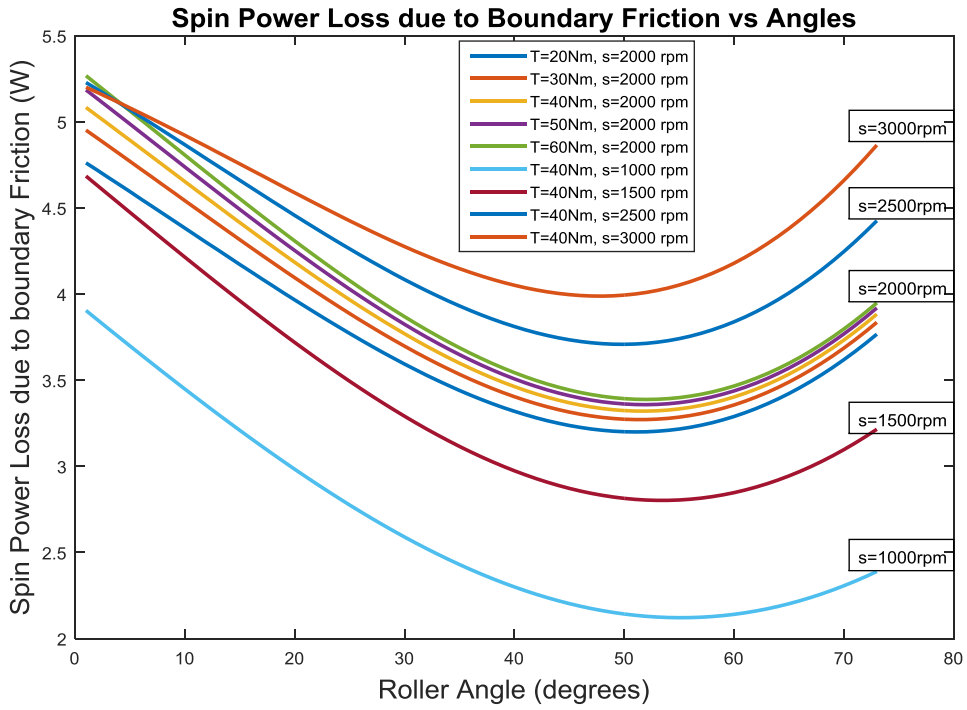

Figure 7- Spin Power loss due to Boundary Friction vs roller

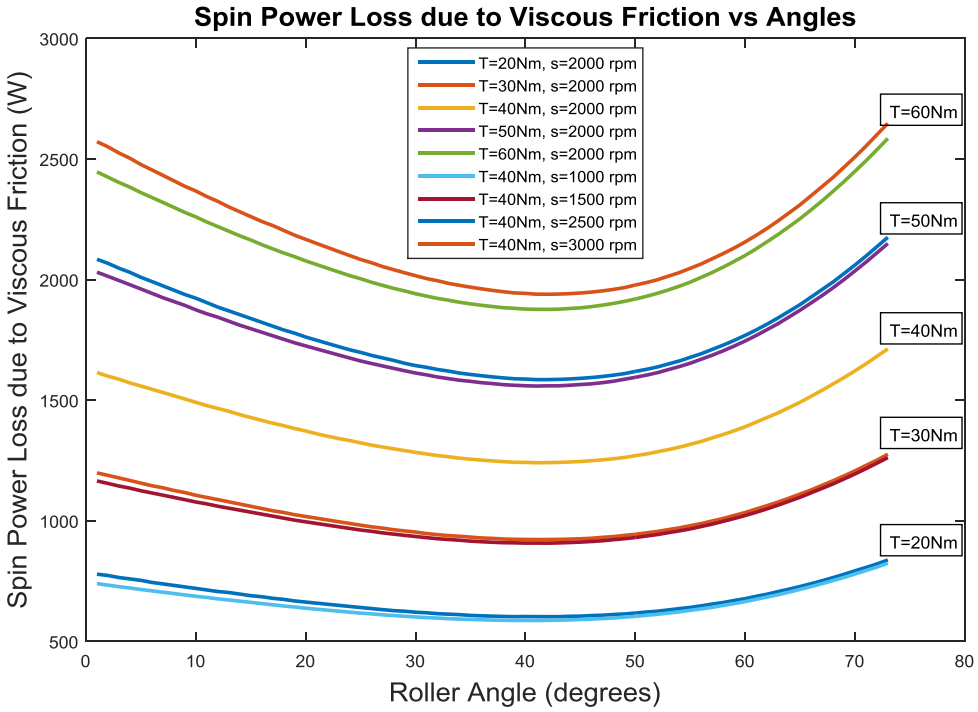

Figure 8- Spin Power loss due to Viscous Friction vs roller angle

4.2. Optimization

Optimisation is carried out with the aim of finding the most efficient combination of materials, lubricant rheology and contact geometry. The following parameters are used: Young's moduli of elasticity, entry lubricant viscosity, and the radii R_{12}, R_{21}, and R_{22} (figure 1). These variables are altered by ±5% of their nominal original values in increments of 2% (giving 6 results per selected parameter). This accounts for 7776 combinations of parameters. The evaluated measures of performance chosen are the resulting mean spin power loss and the mean generated contact pressure.

Table 2 lists the results for the final selected parameter values and the measures of performance with the corresponding percentage changes with respect to the original system configuration.

All the combinations are analysed to obtain the optimum, where the spin power loss would be least simultaneously with a reduced contact pressure. This occurred with the highlighted case (combination number 283), where the contact pressure alters by a mere -2,57% and the spin power loss is reduced by 24.44%, with its share being 419.49W out of the total system parasitic losses of 1716.69 W. This means that the system can be optimized for spin power loss only. As future work, a multi-objective multi-variate optimization should be used in order to optimize the system for all contributing causes to parasitic losses.

Case	Value / %	R12	R22	R21	Entry viscosity	Young modulus [Pa]	Avg power loss	Avg max. pressure
Opt. Number 283	Value	-0,0388 [m]	0,0310 [m]	0,0212 [m]	0,0095 [Pa.s]	199.5 [GPa]	**1297,2 [W]**	2522274899 [GPa]
	Percentage of the original	97	97	105	95	95	**75,56**	97,43

Table 2 – Results of optimization

5. Conclusions

1) The proposed model enables estimation of EHL parameters to be able to aid the design of the CVT.
2) The results show the effect of torque on the required contact load, maximum pressure in the contact and friction which are all affected by the transmitted torque. The lubricant film thickness is least affected because of the prevalent EHL conditions.
3) Film thickness is mostly affected by operational speed, as one would expect under EHL conditions. However, the spin velocity is also affected by the operational speed, which leads to a higher power loss.
4) Results show that nearly 2.5 kW is lost in the system due to the spin power loss. This shows the potential for improvement when working under EHL conditions, which is in line with least contact friction under EHL [4].
5) By altering the applied load, the maximum permissible transmitted torque can be obtained, one which should comply with the maximum permissible contact pressure, which affects the contact fatigue resistance of the materials [6, 7]. The maximum transmitted torque is found to be 60 Nm for the case studied.
6) By altering the bulk rheological properties of the lubricant and materials of the solid boundaries as well as the contact geometry, the system can be optimized for lower spin power loss and reduced contact pressures. The results show that the spin power loss can be reduced by 24%, for minor changes in the contact pressures.

6. References

[1] Chittenden, R. J., Dowson, D. and Taylor, C. M., "Elastohydrodynamic Film Thickness in Concentrated Contacts: Part 2: Correlation of Experimental Results with Elastohydrodynamic Theory", *Proc. IMechE, Part C: J. Mechanical Engineering Science*, 1986, 200(3), pp. 219-226.

[2] Evans, C. R. and Johnson, K. L., "The rheological properties of elastohydrodynamic lubricants. *Proc. IMechE, Part C: J. Mechanical Engineering Science*, 1986, 200(5), pp. 303-312.

[3] Greenwood, J. A. and Tripp, J. H., "The contact of two nominally flat rough surfaces", *Proc. IMechE,* 1970, 185(1), pp. 625-633.

[4]- Gohar, R. and Rahnejat, H., "Fundamentals of Tribology", *Imperial College Press, London,* 2008.

[5]- Johns-Rahnejat, P.M., "Pressure and Stress Distribution under Elastohydrodynamic Point Contacts", *PhD Thesis, Imperial College,University of London*. London, 1988.

[6]- Johns-Rahnejat, P.M. and Gohar, R., "Point contact elastohydrodynamic pressure distribution and sub-surface stress field", In *Tri-Annual Conference on Multi-Body Dynamics: Monitoring and Simulation Techniques,* 1997.

[7] Mohammadpour, M., Theodossiades, S., Rahnejat, H. and Kelly, P., (2013). "Transmission efficiency and noise, vibration and harshness refinement of differential hypoid gear pairs" *Proc. IMechE, Part K: J. Multi-body Dynamics*, 2014, 228(1), pp. 19-33.

[8]- Teodorescu, M., Balakrishnan, S. and Rahnejat, H., "Integrated tribological analysis within a multi-physics approach to system dynamics", *Tribology and interface engineering series*, 2005, 48, pp. 725-737.

[9] Briscoe, B. J. and Evans, D. C. B., "The shear properties of Langmuir-Blodgett layers", *Proc. Roy. Soc. London, Ser. A: Math., Phys. Eng. Sciences,* 1982, 380(1779), pp. 389-407.

[10] Hamrock, B. J. and Dowson, D., "Isothermal elastohydrodynamic lubrication of point contacts: part III—fully flooded results", *Trans. ASME, J. Lubrication Tech.*, 1977, 99(2), pp. 264-275.

Nomenclature

Symbol	Description	Units
A	Apparent contact area (main axis)	m
Aa	Asperity contact area	m^2
A_{cell}	Area of a cell in a grid	m^2
b	Contact area dimension (secondary axis)	m
c'	Specific heat capacity of solid surfaces	J/KgK
dV (i,j)	Vector of speed at a grid-point	m/s
e	Minimum radius of the disk (mid-point)	m

E_1	Young's modulus of the first material	GPa
E_2	Young's modulus of the second material	GPa
E_r	Reduced elastic modulus	Pa^{-1}
f	Angle of spin velocity	degrees
F_2	Statistical function for Gaussian distribution	
$F_{5/2}$	Gaussian distribution of asperities	(-)
f_b	Boundary friction	N
F_{vtotal}	Viscous friction in the contact	N
F_{vcell} (i,j)	Viscous friction in a cell	N
G_e	Materials' parameter	(-)
H^*_{cen}	Dimensionless central film thickness	(-)
h_0	Central film thickness	m
$\boldsymbol{k}$	Ellipticity parameter	(-)
$\boldsymbol{k'}$	Surface material thermal conductivity	W/mK
$\overline{\boldsymbol{k}}$	Lubricant thermal conductivity	$Ns^{-1}{}^{o}C^{-1}$
$n_{contactpoints}$	Number of contact points in the system	(-)
$n_{rollers}$	Number of rollers in the system	(-)
$\overline{\boldsymbol{p}}$	Average pressure	Pa
$\boldsymbol{P}$	Contact pressure	Pa
P_{max}	Maximum Pressure	Pa
P (i,j)	Power loss in a cell	W
P	Pressure	Pa
q	Angle q	degrees
R_{11}	Radius of the disk at the contact point	m
R_{12}	Reduced radius of the disk	m
R_{21}	Reduced radius of the roller	m
R_{22}	Radius of the roller	m
R_{max}	Maximum radius of the disk	m
R_e	Auxiliary orthogonal radii along and normal to V	m
R'	Reduced radius	m
R_s	Auxiliary orthogonal radii along and normal to V	m
R_x	Equivalent principal radii of curvature	m
R_y	Equivalent principal radii of curvature	m
r (i,j)	Moment arm of a cell	m
T	Torque	Nm
U	Rolling speed of disk in the *x*-direction	m/s
U_e	Speed parameter	(-)
V	Inlet lubricant entrainment vector	(-)
v_1	Poisson's ratio of the first material	(-)
v_2	Poisson's ratio of the second material	(-)
ω_{disk}	Angular velocity of the input disk	revs/min
Wa	Asperity load	N

W_e	Load parameter	(-)
Wh	Hydrodynamic load	V
ω_{roller}	Angular velocity of the roller	revs/sec
ω_{spin}	Contact spin velocity	rad/s
W	Contact load	N

Greek symbols

$\boldsymbol{\alpha}$	Pressure-viscosity coefficient	Pa^{-1}
$\overline{\boldsymbol{\alpha}}$	Average pressure coefficient	Pa^{-1}
$\boldsymbol{\beta}$	Average asperity tip radius	m
$\boldsymbol{\varepsilon}$	Slope of the lubricant limiting shear stress–pressure dependence	(-)
$\overline{\boldsymbol{\varepsilon}}$	Simplified elliptical integral	(-)
$\overline{\boldsymbol{\eta}}$	Average viscosity	Pa.s
$\boldsymbol{\eta_0}$	Entry viscosity of the lubricant	Pa.s
$\boldsymbol{\lambda}$	Stribeck's oil film parameter	(-)
$\boldsymbol{\lambda_{cr}}$	Critical Stribeck's parameter	(-)
$\boldsymbol{\mu_m}$	Maximum coefficient of friction	(-)
$\boldsymbol{\sigma}$	Composite RMS surface roughness	m
$\boldsymbol{\rho'}$	Surface material density	kg/m^3
$\boldsymbol{\tau}$	Shear stress	N/m^2
$\boldsymbol{\tau}$ (i,j)	Shear stress at a grid point	N/m^2
$\boldsymbol{\tau_L}$	Limiting shear stress	N/m^2
$\boldsymbol{\tau_0}$	Eyring shear stress	N/m^2
$\overline{\boldsymbol{\tau_0}}$	Average Eyring stress	N/m^2
θ	Angle of entrainment vector	degrees
ξ	Parameter xi	(-)
$\boldsymbol{\xi_1}$	Asperity density per unit area	(-)